Effects of Mutations in Aedes aegypti Sterol Carrier Protein-2 on the Biological Function of the Protein

ARTICLE *in* BIOCHEMISTRY · SEPTEMBER 2010

Impact Factor: 3.02 · DOI: 10.1021/bi902026v · Source: PubMed

3 AUTHORS, INCLUDING:

Q. Lan
University of Wisconsin–Madison
40 PUBLICATIONS **732** CITATIONS

7532 *Biochemistry* **2010,** *49,* 7532–7541
DOI: 10.1021/bi902026v

BIOCHEMISTRY
including biophysical chemistry & molecular biology
Article

Effects of Mutations in *Aedes aegypti* Sterol Carrier Protein-2 on the Biological Function of the Protein[†]

James T. Radek,[‡] David H. Dyer,[§] and Que Lan*[,‡]

[‡]*Department of Entomology, University of Wisconsin, Madison, Wisconsin 53706, and* [§]*Department of Bacteriology, University of Wisconsin, Madison, Wisconsin 53706*

Received November 25, 2009; Revised Manuscript Received August 2, 2010

ABSTRACT: Sterol carrier protein-2 (SCP-2) is a nonspecific intracellular lipid carrier protein. However, the molecular mechanism of ligand selectivity and the *in vivo* function of SCP-2 remain unclear. In this study, we used site-directed mutagenesis to investigate the ligand selectivity and *in vivo* function of the yellow fever mosquito sterol carrier protein-2 protein (AeSCP-2). Mutations to amino acids in AeSCP-2 known to interact with bound ligand also weakened NBD-cholesterol binding. Substitution of amino acids in the ligand cavity changed the ligand specificity of mutant AeSCP-2. Overexpressing wild-type AeSCP-2 in the *Aedes aegypti* cultured Aag-2 cells resulted in an increase in the level of incorporation of [^{3}H]cholesterol. However, overexpressing mutants that were deleterious to the binding of NBD-cholesterol in AeSCP-2 showed a loss of ability to enhance uptake of [^{3}H]cholesterol in cultured cells. Interestingly, when [^{3}H]palmitic acid was used as the substrate for incorporation *in vivo*, there was no change in the levels of incorporation with overexpression of wild-type protein or mutated AeSCP-2s. The *in vivo* data suggest that AeSCP-2 is involved in sterol uptake, but not fatty acid uptake. This is the first report that the cholesterol binding ability may directly correlate with AeSCP-2's *in vivo* function in aiding the uptake of cholesterol.

Sterol carrier protein-2 (SCP-2)[1] is a member of the *SCP-2* gene family that includes genes encoding SCP-2, SCP-x, SCP-like-2, SCP-like-3, 17β-hydroxysteroid dehydrogenase type IV, and stomatin, all of which possess the sterol-binding domain (*1*−*3*). SCP-2 is considered a nonspecific lipid carrier since the vertebrate version of SCP-2 binds to sterols, fatty acids, fatty acid acyl-CoA, and phospholipids (*4*, *5*). However, the molecular mechanisms that underlie SCP-2's ligand selectivity are unknown. The vertebrate SCP-2 has been characterized as a generalized lipid carrier protein thought to mediate cholesterol trafficking and metabolism (*6*) as well as fatty acid uptake and trafficking (*7*). The detailed molecular mechanisms of SCP-2's function, such as whether SCP-2 plays a role in lipid metabolism, lipid uptake, or both, are not well understood. Few data are available to date to show whether ligand binding or ligand selectivity in SCP-2 would impact cellular function.

The yellow fever mosquito, *Aedes aegypti*, sterol carrier protein-2 (AeSCP-2) is strongly expressed in the midgut, the main site of cholesterol absorption, but not in the head and hindgut (*8*). The recombinant AeSCP-2 binds radiolabeled cholesterol with a K_d of 10 nM (*8*). AeSCP-2 has been hypothesized to be involved in the uptake and delivery of cholesterol (an essential nutrient of insects) across the cellular barrier between the midgut and the hemocoel, where it is then transported to sites of either storage or utilization (*8*−*10*). Binding of fatty acid in AeSCP-2 is shown in the protein crystal structure (*9*). AeSCP-2 was localized to the cytosol in the midgut epithelium, and overexpression of the protein in *A. aegypti* cells resulted in an increased level of incorporation of radiolabeled cholesterol (*11*). Knockdown of *AeSCP-2* expression in the last instar larvae resulted in a reduction in the level of cholesterol uptake, higher mortality, and a reduction in fecundity (*10*). In the female adults, knockdown of *AeSCP-2* expression leads to a reduced level of uptake of cholesterol from the blood meal but has little effect on palmitic acid uptake (*2*). In addition, several compounds were discovered from small molecular chemical libraries that inhibited binding of cholesterol to AeSCP-2 (*12*).

Mice with SCP-2 knockout show abnormal metabolism in branched fatty acid and bile acid formation (*13*, *14*), indicating that the mammalian SCP-2 is involved in lipid metabolism. However, the role of SCP-2 in cellular lipid uptake is not clear. Cholesterol can easily insert into the lipid bilayer and has a fast flip-flop rate ($t_{1/2}$ = 1−2 min) within the lipid bilayer (*15*). Diffusion of cholesterol into the lipid bilayer can happen readily, and an aqueous diffusion model has been proposed to account for some of the cholesterol uptake by cells (*16*). However, desorption of membrane-bound cholesterol is slow without the aid of a carrier protein (*3*, *16*). A lipid carrier protein, therefore, enhances desorption of membrane-bound cholesterol through collision with the membrane-bound cholesterol (*17*). Overexpression of the mammalian SCP-2 decreased the plasma membrane content cholesterol in L-cells (*18*), demonstrating the potential of lipid carrier proteins to enhance cellular lipid uptake. There is speculation that the ligand-binding and ligand transfer domains are distinct in SCP-2. The N-terminus of human SCP2 has been

[†]This work was supported by Grant W9113M-05-1-0006 from the Deployed War Fighter Protection Research Program administered by the U.S. Armed Forces Pest Management Board and by National Institutes of Health Grant 5R01AI067422 to Q.L.

*To whom correspondence should be addressed: 1630 Linden Dr., Madison, WI 53706. Telephone: (608) 263-7924. Fax: (608) 262-3322. E-mail: qlan@entomology.wisc.edu.

[1]Abbreviations: AeSCP-2, *Aedes aegypti* sterol carrier protein-2; SCPI, *A. ageypti* sterol carrier protein-2 inhibitor; DTT, dithiothreitol; EDTA, ethylenediaminetetraacetic acid; GST, glutathione *S*-transferase; SCP-2, sterol carrier protein-2; NBD-cholesterol, 22-[*N*-(7-nitrobenz-2-oxa-1,3-diazol-4-yl)amino]-23,24-bisnor-5-cholen-3β-ol.

 Published on Web 08/03/2010

shown to be a membrane interaction domain (*19*). On the other hand, a single point mutation in *Arabidopsis thaliana* SCP-2 from Met100 to Leu100 abolished sterol binding (*20*).

Using the X-ray crystallographic structure of AeSCP-2 and its palmitic acid-binding domain as a template (*9*), mutants of *AeSCP-2* were created and studied for their ability to interact with ligands. In addition, cultured *A. aegypti* cells were transfected with overexpression vectors of *AeSCP-2* wild type and mutants and tested for their abilities to enhance incorporation of either radiolabeled cholesterol or palmitic acid. In their natural environment, *A. aegypti* larvae feed on detritus which would include various sterols such as cholesterol, phytsterols, and fungal sterols. Little is known about whether AeSCP-2 is involved in dietary sterol uptake or metabolism in mosquitoes. We report here for the first time that the binding of β-sitosterol, but not of 7-dehydrocholesterol, in AeSCP-2 occurs *in vitro*, and the selectivity of the ligand can be altered via single-point mutation that may affect the ligand cavity in the protein. Furthermore, the *in vivo* function of AeSCP-2 may be complex because of the selectivity in AeSCP-2-mediated cellular uptake of ligands. These results extend our knowledge of these critical interactions between AeSCP-2 and ligands as well as inhibitors.

MATERIALS AND METHODS

Chemicals and Instrumentation. Chemicals and reagents were purchased from Sigma (St. Louis, MO), Fisher Scientific (Pittsburgh, PA), and ICN (Costa Mesa, CA) if their origins are not mentioned in the text. NBD-cholesterol was purchased from Molecular Probes (Eugene, OR). [1,2-^{3}H(N)]Cholesterol (40 Ci/mmol) and [9,10-^{3}H]palmitic acid (60 Ci/mMol) were purchased from American Radiolabeled Chemicals, Inc. (St. Louis, MO). AeSCP-2 inhibitors, SCPI-1 (*N*-4-{[4-(3,4-dichlorophenyl)-1,3-thiazol-2-yl]amino}phenyl)acetamide hydrobromide) and SCPI-2 [8-chloro-2-(3-methoxyphenyl)-4,4-dimethyl-4,5-dihydroisothiazol-[5,4-*c*]quinoline-1(2*H*)-thione], were purchased from ChemBridge Corp. (San Diego, CA) at at least 90% purity.

All fluorescence measurements were performed in a SpectraMax GeminiXS microplate fluorometer (Molecular Devices, Sunnyvale, CA) or a Synergy HT Multi-Detector Microplate Reader (BIO-TEK Instruments, Winooski, VT). Radiolabeled measurements were taken in a 2500 TR liquid scintillation analyzer (Canberra, Meriden, CT).

Cell Culture. The *A. aegypti* cell line (Aag-2) was maintained in Eagle's medium (Invitrogen, Carlsbad, CA) supplemented with 5% fetal bovine serum (E5 complete medium) and grown at 28 °C in a 5% CO_2 atmosphere (*21*, *22*). Cells were passed every 7 days in a 1:4 dilution of cells.

Plasmid Construction and Purification. Recombinant AeSCP-2 was expressed using a pGEX-4T-2 plasmid with the entire coding sequence of AeSCP-2 cloned in as previously described (*9*). For overexpression of AeSCP-2 in Aag-2 cells, the entire coding region of AeSCP-2 was inserted into the pIE1^{hr} expression vector (gift of P. Frisson of the University of Wisconsin) using *Hin*dIII and *Bgl*II sites in the multiple-cloning region. The plasmids were purified using the Maxiprep kit (Qiagen, Valencia, CA). The quantity of DNA was determined by measurement of the UV spectrum at 260 nm.

Site-Directed Mutagenesis. Mutations in the pGEX-4T-2/AeSCP-2 and pIE1^{hr}/AeSCP-2 plasmids were introduced using the QuikChange II site-directed mutagenesis kit (Stratagene, La Jolla, CA). Mutant plasmids were sequenced to confirm the introduced point mutations using an automatic sequencer (ABI 377XL) and Big Dye labeling (American Pharmacia Biotech AB, Uppsala, Sweden).

Recombinant Protein Expression and Purification. The recombinant *AeSCP-2* wild type and mutants were expressed and purified as described previously (*9*) with the following changes. Purified samples of recombinant proteins were concentrated in either 50 mM Tris-HCl (pH 8.0) or 10 mM K_2PO_4 (pH 7.5) in CENTRIPREP centrifugal filter devices [10K cutoff (Amicon, Billerica, MA)] to a final volume of 1 mL after reconcentration of the sample from 10 mL of buffer 10 times. A sample (0.5 mg) of AeSCP-2 was dialyzed against 4 × 4 L of ddH_2O, then lyophilized, and subjected to mass spectroscopy in a Voyager DE-Pro MALDI-TOF mass spectrometer (Applied Biosystems, Foster City, CA) to demonstrate that purified AeSCP-2 was in the apo form. The protein concentration was determined using Coomassie Plus-The Better Bradford Assay Kit (Pierce, Rockford, IL) using bovine serum albumin as a standard. The purification of recombinant AeSCP-2 wild type and mutants was monitored by Western blot analysis using an antibody raised against recombinant AeSCP-2 (*8*). All mutants of AeSCP-2 used in this study were recognized by the antibody and were similarly purified to homogeneity (data not shown).

Purified recombinant proteins were subjected to dynamic light scattering to determine whether the purified protein was in the monomeric state. AeSCP-2 wild type binds to ligand as a monomer (*9*); the soluble state of the protein was a concern because mutation in a protein may cause the instability of the protein structure that would result in aggregation of the protein. Dynamic light scattering (DLS) experiments were performed with a DynaPro (Protein Solutions, Santa Barbara, CA) in a 12 μL quartz cuvette at 23 °C. Protein samples buffered in PBS [137 mM NaCl, 2.7 mM KCl, 10 mM dibasic sodium phosphate, and 2 mM monobasic potassium phosphate (pH 7.4)] were concentrated to approximately 1 mM and passed through a 0.22 μM spin filter at 3000*g* for 3 min. Samples were stored on ice prior to the DLS measurements. The hydrodynamic radius, polydispersity, and presence of aggregates were analyzed for each mutant as well as wild-type recombinant AeSCP-2s. DLS has been used extensively to demonstrate a protein sample is free of major aggregates prior to the investment of time in crystallization trials (*23*). The proteins analyzed in this study exhibited a narrow unimodal distribution with polydispesity ranging from ≤30%, thereby demonstrating the protein samples were well folded and not in an aggregated state.

Binding of NBD-Cholesterol to AeSCP-2. The binding of 0.5 μM NBD-cholesterol in 50 mM Tris-HCl (pH 8.0) at 25 °C to increasing concentrations of either AeSCP-2 wild type or mutants was monitored by fluorescence spectroscopy. Sample volumes were 100 μL. Excitation was at 470 nm, and emission was measured at 530 nm. Difference spectra were generated from the subtraction of buffer and ligand/inhibitor spectra without protein from the protein/ligand/inhibitor sample spectra. K_d values were obtained with data using a simple, single-binding site, nonlinear regression model in GraphPad Prism version 4.0 (GraphPad Software Inc., San Diego, CA) using the equation

$$Y = \frac{B_{max}X}{K_d + X}$$

Ligand Competition Assays. For initial ligand competition assays (Figure 1), increasing concentrations of a competitor (cholesterol, 7-dehydrocholesterol, palmitic acid, or β-sitosterol)

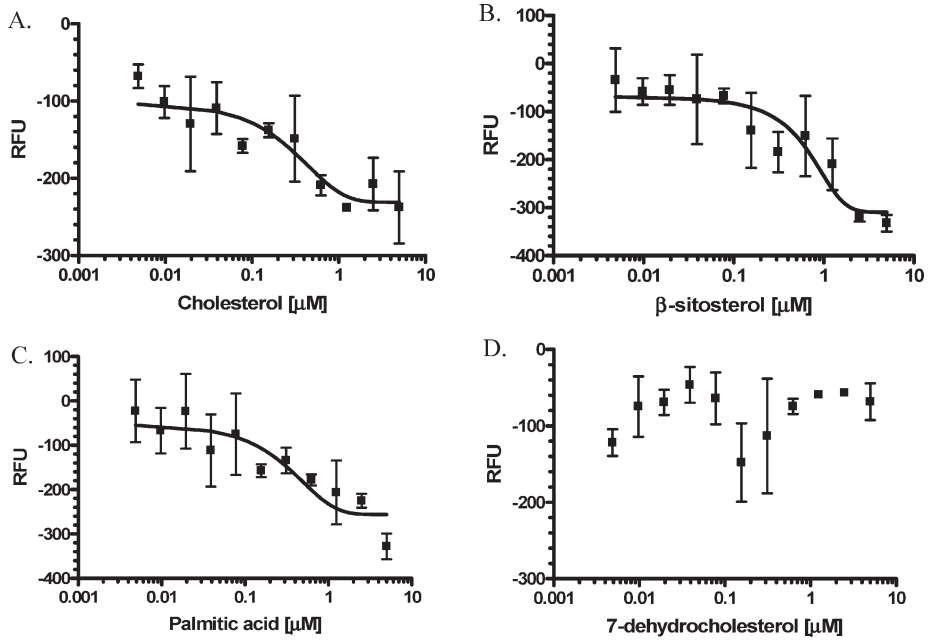

FIGURE 1: Binding of NBD-cholesterol (1.25 μM) to AeSCP-2 in the presence of a competitive ligand (0.005−5 μM): (A) cholesterol, (B) β-sitosterol, (C) palmitic acid, and (D) 7-dehydrocholesterol. The background NBD-cholesterol fluorescence (NBD-cholesterol alone in the reaction buffer) was deducted from each assay. The trend line (the slope was shown by the trend line) was drawn from the mean of three replicates, and the bars represent the standard deviation.

Table 1: NBD-Cholesterol Binding to Wild-Type AeSCP-2 in the Presence of a Competitive Ligand[a]

	0 μM competitor	0.1 μM competitor			2 μM competitor		
	K_d (μM)[b]	K_d (μM)[b]	mean difference[c] vs [0]	P[c]	K_d (μM)[b]	mean difference vs [0]	P
cholesterol	0.99 (0.21)	3.77 (0.74)	58.27	< 0.01	7.36 (2.07)	50.07	< 0.01
palmitic acid	0.99 (0.21)	11.32 (3.90)	67.92	< 0.01	9.9 (3.49)	51.15	< 0.01
β-sitosterol	0.99 (0.21)	5.45 (2.11)	48.79	< 0.01	5.51 (0.81)	39.16	> 0.05
7-dehydrocholesterol	0.99 (0.21)	1.92 (0.81)	30.22	> 0.05	1.35 (0.38)	5.624	> 0.05

[a]Net changes in NBD-cholesterol fluorescence intensity (RFU, relative fluorescence unit) of 0.1 μM NBD-cholesterol and increasing concentrations of wild-type recombinant AeSCP-2 (0.02−20 μM) in the presence of a competitor. [b]Mean K_d values of three replicates and the standard error are shown. [c]The K_d values were compared using a repeated measures analysis of variance followed by Dunnett's post test, and mean differences of the Dunnett's multiple-comparison test between the absence and presence of a competitor are shown.

Table 2: Difference between Wild-Type AeSCP-2 and Mutants in NBD-Cholesterol Binding *in Vitro*[a]

	wild type	Y30A	F9W/W44F	F105A	F105W	M90L	W44E	F32W	F32A
K_d (μM)[b]	0.34 (0.16)	0.25 (0.05)	0.91 (0.62)	1.15 (0.09)	1.32 (0.45)	2.75 (1.45)	4.20 (1.67)	4.94 (1.59)	6.36 (2.11)
P[c] vs wild type	−	> 0.05	> 0.05	> 0.05	> 0.05	> 0.05	> 0.05	> 0.05	< 0.05
x-fold change in K_d		0.73	2.68	3.38	3.88	8.09	12.35	14.53	18.71

[a]Net changes in NBD-cholesterol fluorescence intensity (RFU) at each concentration were processed [0.5 μM NBD-cholesterol with increasing protein concentrations (from 0.01 to 10 μM)]. [b]Mean K_d values (standard deviation) determined using the GraphPad Prism version 4.0 (single-binding site, nonlinear regression model). [c]P values were given for Dunnett's post test between the wild type and each mutant after a repeated measures analysis of variance.

were added to 100 μL samples of 5 μM AeSCP-2 and 10 μM NBD-cholesterol in 10 mM KPO_4 (pH 7.5) at 25 °C. Samples in 96-well plates were measured in the microplate fluorometer.

For binding assays, 0.1 and 0.5 μM NBD-cholesterol (Tables 1 and 2, respectively) and increasing concentrations of wild-type recombinant AeSCP-2 (0.02−20 μM) were mixed together in the presence of a competitor. Excitation was at 470 nm, and emission was measured at 530 nm. Difference spectra were generated from the subtraction of buffer and ligand/inhibitor spectra without protein from the protein/ligand/inhibitor sample spectra. The results are the average of three experiments with standard deviations.

For ligand competition assays with NBD-cholesterol in the presence of wild-type AeSCP-2 or an AeSCP-2 mutant (Table 3), the 50% effective concentration (EC_{50}) was obtained using a single-site competition, nonlinear regression model in GraphPad Prism version 4.0 (GraphPad Software Inc.) using the equation

$$Y = \frac{\text{best fit value MIN} + \text{best fit value MAX} - \text{best fit value MIN}}{1 + 10^{X - \log EC_{50}}}$$

In Vivo Incorporation of [^{3}H]Cholesterol by Cells Over-expressing AeSCP-2 Wild Type and Mutants. The Aag-2 cells were grown to 40% confluence in a 65 mm tissue culture dish

Table 3: Effects of Point Mutations in AeSCP-2 on Competitive Binding of Ligands [EC_{50} (μM)][a]

competitor/protein	EC_{50}	EC_{50} with 90% confidence interval	Dunnett's test[b]	mean difference	*P* value
cholesterol/wild type	0.211	0.01760 to 2.544	wild type		
cholesterol/Y30A	0.282	0.05466 to 1.452	vs Y30A	−24.82	> 0.05
cholesterol/F32W	0.447	0.09762 to 2.049	vs F32W	−68.86	< 0.01
cholesterol/W44A	0.072	0.02259 to 0.2292	vs W44A	−6.014	> 0.05
cholesterol/W44E	ND		vs W44E	57.24	< 0.01
cholesterol/M90L	ND	8.003×10^{-16} to 3.009×10^{8}	vs M90L	35.35	< 0.05
cholesterol/F105W	0.474	0.009708 to 23.14	vs F105W	38.39	< 0.01
β-sitosterol/wild type	0.142	0.002813 to 7.203	wild type		
β-sitosterol/Y30A	0.096	0.01598 to 0.5792	vs Y30A	−53.42	< 0.01
β-sitosterol/F32W	0.061	0.002376 to 1.591	vs F32W	−58.36	< 0.01
β-sitosterol/W44A	0.112	0.007834 to 1.607	vs W44A	−6.309	> 0.05
β-sitosterol/W44E	0.042	0.003440 to 0.5018	vs W44E	130.1	< 0.01
β-sitosterol/M90L	0.046	0.005384 to 0.3945	vs M90L	128.7	< 0.01
β-sitosterol/F105W	0.083	0.008206 to 0.8347	vs F105W	74.13	< 0.01
palmitic acid/wild type	0.348	0.06839 to 1.767	wild type		
palmitic acid/Y30A	0.100	0.02338 to 0.4259	vs Y30A	−23.67	> 0.05
palmitic acid/F32W	0.398	0.1225 to 1.291	vs F32W	−88.96	< 0.01
palmitic acid/W44A	0.127	0.03991 to 0.4065	vs W44A	−23.87	> 0.05
palmitic acid/W44E	0.075	0.01329 to 0.4237	vs W44E	2.003	> 0.05
palmitic acid/M90L	0.127	0.03367 to 0.4777	vs M90L	66.14	< 0.01
palmitic acid/F105W	0.175	0.04578 to 0.6685	vs F105W	26.4	> 0.05
7-dehydrocholesterol/wild type	ND		wild typet		
7-dehydrocholesterol/Y30A	0.191	0.02403 to 1.513	vs Y30A	−54.77	< 0.01
7-dehydrocholesterol/F32W	0.260	0.005156 to 13.09	vs F32W	−75.19	< 0.01
7-dehydrocholesterol/W44A	ND		vs W44A	−24.45	> 0.05
7-dehydrocholesterol/W44E	ND	0.0005127 to 1364	vs W44E	52.63	< 0.01
7-dehydrocholesterol/M90L	ND	2.143e-006 to 6354	vs M90L	43.4	< 0.01
7-dehydrocholesterol/F105W	ND		vs F105W	6.76	> 0.05

[a] EC_{50} value (50% maximal effective concentration): mean and 95% confidence interval (CI). ND means the EC_{50} value could not be determined because of "not converge" or extremely wide ranges of the EC_{50} 95% CI (≥4 orders of magnitude). The average values of net changes in NBD-cholesterol fluorescence intensity (RFU) of four independent samples were processed using GraphPad Prism version 4.0 (single-competition site, nonlinear regression model). [b] Mutant and wild-type EC_{50} values were compared using a repeated measures analysis of variance followed by Dunnett's post test.

in E5 complete medium. Cells were transfected with 12 μg of an overexpression plasmid and 24 μL of Lipofectin/mL for 8 h in the transfection medium (E5 complete medium without FBS and antibiotics). Cells were then transferred to E5 complete medium. Thirty-six hours after transfection, the cells were transferred to steroid-free E5 complete medium (*24*) for 12 h. Medium was replaced with 1 mL of steroid-free E5 complete medium containing either 0.33 μCi of [^{3}H]cholesterol/mL or 0.33 μCi of [^{3}H]palmitic acid/mL and incubated for 12 h. The labeled cells were gently washed twice in 2 mL of cold PBS in the dish. Lipids were extracted from the cells, and the radioactivity in each sample was measured in a liquid scintillation counter as described previously (*6*). The protein pellets from each sample were redissolved in 200 μL of PBS, and protein concentrations were determined using the BCA kit (Pierce).

To quantify the overexpression of AeSCP-2 and mutants, an indirect enzyme-linked immunosorbent assay (ELISA) was performed in a 96-well microtiter plate using an antibody raised in a rabbit against purified recombinant AeSCP-2. Protein samples (100 μL/well) from Aag-2 cells were loaded into a 96-well plate (immunoassay microplate, Thermo Scientific, Waltham, MA) and incubated for 1 h at room temperature. The samples were removed, and a 200 μL solution of blocking buffer (10 mg/mL bovine serum albumin and 1% goat serum) was added and incubated for 1 h at room temperature. The primary antibody to AeSCP-2 (1:2000 in 100 μL of PBS/well) was shaken in for 1 h at room temperature. The wells were washed in a PBS/0.1% Tween 20 solution three times, and the secondary antibody (goat antirabbit IGG) was added (1:2000 in 100 μL) and incubated for 1 h at room temperature. The wells were washed in a PBS/0.1% Tween 20 solution three times, and a 100 μL solution of 1.8 mM 2,2′-azinobis(3-ethylbenzthiazoline-6-sulfonic acid) was added to each well. The plates were read in a VERSAmax microplate reader (Molecular Devices) at 405 nm. Purified recombinant AeSCP-2 in PBS was used in a concentration range of 0−1 μM to generate a standard curve. There were no significant differences in the levels of overexpressed AeSCP-2 and mutant in different samples of transfected Aag-2 cells (Table 1 of the Supporting Information). Therefore, the content of a ^{3}H-labeled lipid is described as disintegrations per minute per milligram of total cellular protein.

Intrinsic Fluorescence Measurements of SCPIs Bound to AeSCP-2 Wild Type and Mutants. Fluorescence measurements from intrinsic sources are often useful for reporting conformational states of proteins (*25*). Fluorescence emission from tryptophan (Trp) residues in a protein is extremely sensitive to perturbations in the local environment, mostly due to different degrees of quenching. AeSCP-2 has only one tryptophan residue at position 44 that is mostly buried in the hydrophobic core of the protein [Figure 3 of the Supporting Information (*9*)]. Recombinant protein samples of the wild type and mutants (20−50 μM) in a 96-well microplate were measured for their intrinsic fluorescence intensities in the absence and presence of either SCPI-1 or SCPI-2 (50−100 μM). SCPI-1 and SCPI-2 are two AeSCP-2 inhibitors identified via high-throughput screening for AeSCP-2 chemical inhibitors (*12*). Sample volumes were 100 μL in 50 mM Tris-HCl (pH 8.0) at 25 °C. The samples were excited at 280 nm, and emission spectra were recorded from 320 to 390 nm.

Difference spectra were generated by the subtraction of buffer and SCPI alone spectra from the protein spectra.

To ensure that the quenching of intrinsic tryptophan fluorescence was due to the interaction of inhibitor and the tryptophan in the native state of the protein, negative control spectra were recorded after proteins were denatured in 6.5 M guandidine-HCl in 50 mM Tris-HCl (pH 7.4).

Statistical Analysis. Binding or competitive binding assays presented in each table were always performed in parallel with three or four independent replicates. Therefore, K_d and EC_{50} values were compared using a repeated measures analysis of variance followed by Dunnett's post test using GraphPad Prism version 4.0 (GraphPad Software Inc.) unless otherwise indicated. The data in this study were analyzed using a statistical method similar to that described by others reporting similar studies on point mutation and ligand interactions (*26*).

RESULTS

Ligand Binding and Competition in AeSCP-2. NBD-cholesterol is a fluorescent analogue of cholesterol that has little fluorescence in hydrophilic solutions. After NBD-cholesterol binds to a protein in the hydrophobic cavity of the protein, its fluorescence intensity increases. NBD-cholesterol has been used as the probe in studying sterol-binding proteins (*27*). Cholesterol has been shown to compete with NBD-cholesterol for binding to AeSCP-2 (*12*). Palmitic acid and cholesterol have been shown to bind AeSCP-2 (*8*, *9*). Earlier reports show that *A. aegypti* larvae readily convert β-sitosterol to cholesterol (*28*, *29*), whereas conversion of cholesterol to 7-dehydrocholesterol is the first step in the steroid hormone biosynthesis pathway (*30*). It is known that the vertebrate SCP-2 is a nonspecific intracellular lipid carrier (*3*). Therefore, potential competitors for binding in AeSCP-2 could be cholesterol, 7-dehydrocholesterol, palmitic acid, and β-sitosterol. Here we show that in addition to cholesterol, other ligands competed with the fluorescent cholesterol analogue for binding to AeSCP-2. Cholesterol competed with the NBD-cholesterol for binding to AeSCP-2 in a dose-dependent fashion (Figure 1A, cholesterol), consistent with what has been reported previously (*12*). In addition, palmitic acid and β-sitosterol also competed with NBD-cholesterol for binding to AeSCP-2 (panels B and C of Figure 1 for β-sitosterol and palmitic acid, respectively). Interestingly, 7-dehydrocholesterol did not appear to compete with NBD-cholesterol for binding to AeSCP-2 (Figure 1D, 7-*d*-cholesterol), suggesting that AeSCP-2 may not bind this metabolite of cholesterol. To further verify the potential ligands for AeSCP-2, NBD-cholesterol (0.1 μM) binding was measured with recombinant wild-type AeSCP-2 with increasing protein concentrations (0.02−20 μM) in the presence of a competitor. At 5 μM AeSCP-2 and 0.1 μM NBD-cholesterol, the fluorescence intensity of bound NBD-cholesterol had reached a maximal level (Figure 2 of the Supporting Information). In the presence of a specific competitor under the same conditions, the level of binding of NBD-cholesterol would be reduced which would appear as an increase in the K_d value for NBD-cholesterol compared to that in the absence of a competitor. The level of binding of NBD-cholesterol to AeSCP-2 was reduced significantly in the presence of $\geq$0.1 μM palmitic acid and cholesterol (Table 1). The results suggest that cholesterol and palmitic acid might be natural ligands for AeSCP-2. On the other hand, significant reductions of K_d values were detected only at 0.1 μM for β-sitosterol (Table 1, β-sitosterol), indicating β-sitosterol might be a natural ligand for AeSCP-2. However, the presence of 7-dehydrocholesterol did not significantly alter the K_d values under the same conditions (Table 1, 7-dehydrocholesterol), indicating 7-dehydrocholesterol might not be a specific competitive ligand for AeSCP-2. The results showed that cholesterol, palmitic acid, and β-sitosterol were likely ligands of AeSCP-2. This is the first report of β-sitosterol as a potential AeSCP-2 ligand.

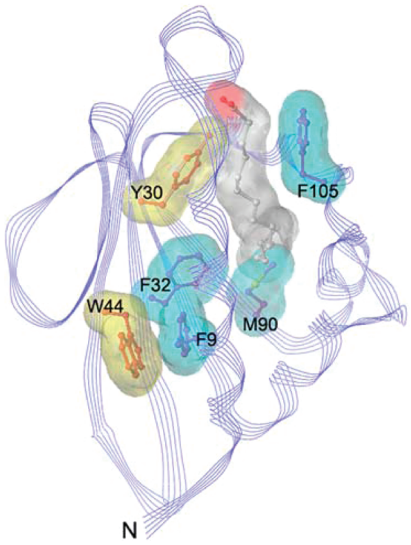

FIGURE 2: Ribbon diagrams (Sybyl) of AeSCP-2 (Protein Data Bank entry 1PZ4) at 1.35 Å resolution and selected amino acid residues for point mutations that directly interact with the bound ligand (blue colored sticks; F9, F32, M90, and F105) and that are not in direct contact with the ligand (orange colored stick; Y30 and W44). The C16 fatty acid is highlighted as a ball and stick model with carbons (white) and oxygen (red).

Ligand Binding in AeSCP-2 Mutants. The three-dimensional protein structure of AeSCP-2 shows that hydrophobic amino acid residues line the interior ligand-binding cavity (*9*). On the basis of the protein structure of AeSCP-2, we selected several amino acid residues (Figure 2, F9, Y30, F32, W44, M90, and F105) in AeSCP-2 for point mutation experiments to shed light on the mechanism of ligand binding in AeSCP-2. The Y30 residue does not directly interact with bound ligand, although Y30 resides in the hydrophobic core of the protein (*9*), whereas the only tryptophan residue at position 44 seems to form $\pi-\pi$ stocking with F9 that may stabilize the ligand cavity (*1*). All of the point mutations except Y30A in AeSCP-2 caused reductions in the level of binding of NBD-cholesterol (Figure 3). Wild-type AeSCP-2 and the Y30A mutant have K_d values for NBD-cholesterol of 0.34 and 0.25 μM, respectively (Table 2). Mutations F9W/W44F, F105A, F105W, F32A, F32W, W44E, and M90L in AeSCP-2 weakened the ability of the mutants to bind NBD-cholesterol compared to that of the wild type (Figure 3 and Table 2). However, the F32W mutant was the only mutant that caused significant changes in K_d values compared to the wild type (Table 2). Mutant F32W reduced NBD-cholesterol binding affinity by more than 10-fold (Table 2), which also significantly decreased the sensitivity to cholesterol competitive binding (Table 3). Interestingly, mutants that resulted in only moderate reductions in the level of NBD-cholesterol binding (Table 2) had severely affected the sensitivity to cholesterol binding (Table 3). Both W44E and M90L lost the ability to bind cholesterol competitively but retained palmitic acid binding capacity (Table 3). These results further established that AeSCP-2 binds NBD-cholesterol and that critical amino acids in the protein structure,

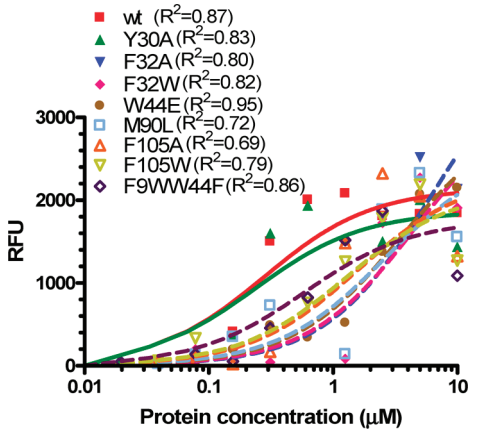

FIGURE 3: Binding of NBD-cholesterol to recombinant wild-type and mutant AeSCP-2s. The background NBD-cholesterol fluorescence (NBD-cholesterol alone in the reaction buffer) was deducted from each assay. Shown are net changes in NBD-cholesterol fluorescence in intensity (RFU, relative fluorescence unit) at 0.5 μM in the presence of increasing concentrations of each protein (from 0.01 to 10 μM). The data represent mean values from three replicates and were processed using GraphPad Prism version 4.0 (single-binding site, nonlinear regression model). R^2 values of each nonlinear regression curve are shown.

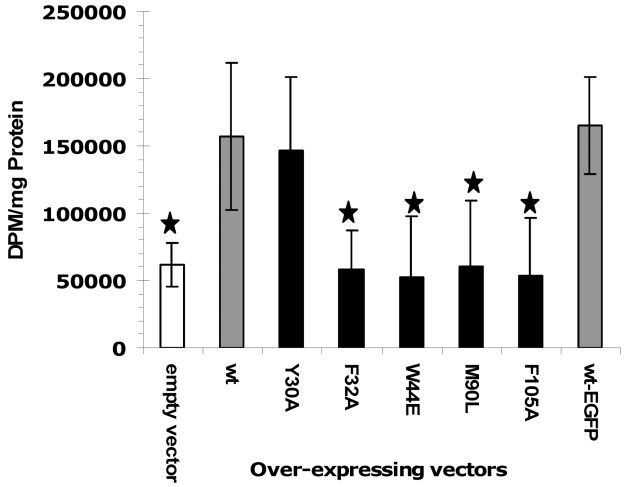

FIGURE 4: Effect of point mutations in AeSCP-2 on [^{3}H]cholesterol uptake in *A. aegypti* Aag-2 cells. Aag-2 cells were transfected with overexpression vectors (see Materials and Methods), and the empty vector was used as a negative control. Overexpression of each protein was verified via Western blotting analysis (Figure 2 of the Supporting Information). The mean and standard deviation are shown (N = 3). Stars denote significant differences (p < 0.05) between wild-type AeSCP-2 and mutant AeSCP-2s and the negative control.

when changed, appeared to be responsible for the reduced binding affinity for the ligand. It is interesting to note that all mutant AeSCP-2s studied bound NBD-cholesterol at higher concentrations of the protein (Figure 3, ≥5 μM proteins), suggesting that none of the individual amino acid mutations were sufficiently severe to abolish binding of NBD-cholesterol to the protein.

To investigate whether point mutations in AeSCP-2 also affect ligand binding specificity, we used the mutant AeSCP-2s to perform competitive binding assays. We performed competitive binding assays with 5 μM purified protein and 1.25 μM NBD-cholesterol under conditions of increasing concentrations of a competitor. In wild-type AeSCP-2, the only ligand that did not show competitive binding was 7-dehydrocholesterol (Table 3), which is consistent with previous results (Table 1 and Figure 1). There was little change in the competitive binding of palmitic acid in tested mutants (Table 3, palmitic acid). However, in mutants M90L and W44E, cholesterol lost its ability to bind competitively to the proteins (Table 3). On the other hand, β-sitosterol was able to compete with NBD-cholesterol for binding to M90L and W44E (Table 3). Interestingly, Y30A and F32W mutations enabled 7-dehydrocholesterol to compete with NBD-cholesterol for binding to the proteins (Table 3), whereas wild-type AeSCP-2 did not (Figure 1 and Tables 1 and 3). The results indicate that cholesterol and palmitic acid, two ligands that are known to bind to AeSCP-2 (*8*, *9*), may be accommodated via different amino acid residues in AeSCP-2.

In Vivo Function of AeSCP-2 Mutants. Studies of the incorporation of radiolabeled cholesterol and palmitic acid into cells were conducted using *A. aegypti* cell line Aag-2 that is embryonic in origin (*31*). The mosquito cells were transfected with overexpression vectors of either wild-type or mutant AeSCP-2s, and the AeSCP-2-overexpressing cells were then incubated with labeled ligand. Previously, the level of incorporation of [^{3}H]cholesterol was shown to increase in cells overexpressing AeSCP-2 (*11*). To determine if the mutations in AeSCP-2 that exhibited reduced affinity for cholesterol *in vitro* (Figure 3 and Table 2) or impaired competitiveness for cholesterol binding (Table 3) would have any effect on AeSCP-2's function *in vivo*, expression vectors were constructed to overexpress AeSCP-2 mutants in Aag-2 cells. The level of incorporation of [^{3}H]cholesterol increased significantly compared to that of the empty vector when wild-type AeSCP-2 was overexpressed in the Aag-2 cells (Figure 4, wt vs empty vector), which was consistent with previously reported studies (*11*). Overexpressing the wild-type AeSCP-2−EGFP fusion protein led to similar levels of [^{3}H]cholesterol incorporation compared to that of wild-type AeSCP-2 (Figure 4, wt-EGFP vs empty vector), indicating that the EGFP tag at the C-terminus of wild-type AeSCP-2 did not affect the *in vivo* function of AeSCP-2. However, the level of incorporation of [^{3}H]cholesterol did not increase in cells overexpressing AeSCP-2 mutants F32A, W44E, M90L, and F105A when compared to that of the wild type (Figure 4). On the other hand, overexpression of the Y30A mutant had increased levels of [^{3}H]cholesterol incorporation similar to that of wild-type AeSCP-2 (Figure 4). The Y30A mutation had little effect on the binding of cholesterol to the protein *in vitro* or sensitivity for cholesterol competitive binding (Figure 3 and Tables 2 and 3), whereas F32A, W44E, M90L, and F105A mutants exhibited moderately decreased affinity for NBD-cholesterol (Figure 3 and Tables 2 and 3), and W44E and M90L lost sensitivity for cholesterol competitive binding. The results indicate that cholesterol binding in AeSCP-2 directly correlated with the *in vivo* function of AeSCP-2 in enhancing cholesterol uptake.

In contrast, when [^{3}H]palmitic acid was used as the ligand, there was no increase in the level of [^{3}H]palmitic acid incorporation when the cells were transfected with either empty or AeSCP-2 wild-type expression vectors (Figure 5). The results are consistent with a previous report that shows overexpression of wild-type AeSCP-2 did not enhance [^{3}H]palmitic acid uptake in cultured cells (*31*). Overexpression of AeSCP-2 mutants in Aag-2 cells did not affect [^{3}H]palmitic acid incorporation (Figure 5). The results suggest that AeSCP-2 does not play a significant role in palmitic acid incorporation in the Aag-2 cells, despite the fact that palmitic acid bound specifically to AeSCP-2 and the mutants *in vitro* (Figure 1 and Tables 1 and 3).

Effects of SCPIs on Intrinsic Trp Fluorescence. Both SCPI-1 and SCPI-2 suppress NBD-cholesterol binding in AeSCP-2 at an IC_{50} of <0.4 μM (*12*). However, molecular interactions between AeSCP-2 and SCPIs are unclear. Whether SCPIs bind to AeSCP-2 like the natural ligand is unknown. The intrinsic fluorescent emission of the Trp residue in proteins is sensitive to perturbations in the local environment, due mostly to different degrees of quenching. A Trp residue buried in a hydrophobic domain of a native protein has its maximal fluorescence intensity usually at 330−333 nm, whereas in a denatured protein, the Trp residue's fluorescence emission shows a red shift to 350−353 nm (*32*). AeSCP-2 has only one tryptophan residue that is situated within the hydrophobic ligand binding cavity, though it does not directly interact with the ligand (*9*). Wild-type recombinant AeSCP-2 exhibited a tryptophan fluorescence emission peak at ~332 nm (Figure 6A, AeSCP-2 wt), indicating that the W44 residue is most likely buried in a hydrophobic domain. In the presence of either 50 μM SCPI-1 or 50 μM SCPI-2, there is a significant decrease in the tryptophan intrinsic fluorescence signal of wild-type AeSCP-2 at 10 μM (Figure 6A, AeSCP-2 wt + SCPI-1 or + SCPI-2). The quenching effects of SCPI-1 on intrinsic fluorescence of Trp in wild-type AeSCP-2 were consistent with that of an earlier report (*33*). However, this is the first report that SCPI-2 quenched Trp intrinsic fluorescence in wild-type AeSCP-2 in a fashion similar to that of SCPI-1. In contrast, cholesterol does not produce a quenching of the intrinsic Trp fluorescence signal in AeSCP-2 (Figure 6A, AeSCP-2 wt + cholesterol). For negative controls, the protein was denatured in 6.5 M guanidine hydrochloride and had a tryptophan intrinsic fluorescence emission peak at 352 nm that is typical of Trp fluorescence in denatured protein (*32*), showing no significant quenching of the signal in the presence of SCPI-1 or SCPI-2 (Figure 6B). These data suggested a strong link of inhibitor binding in a region close to an intrinsically fluorescing amino acid. The most likely candidate for this interaction is the single tryptophan at position 44 (W44) in the polypeptide chain. Interestingly, SCPI-1 still quenched the tryptophan intrinsic fluorescence in mutants F9W/W44F and M90L (Figure 6C,D, SCPI-1), whereas SCPI-2 did not affect the intrinsic fluorescence of W44 in the same mutants (Figure 6C,D, SCPI-2).

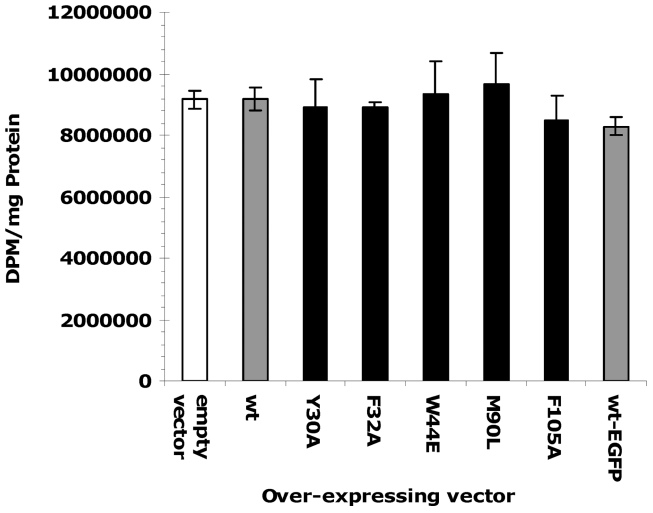

FIGURE 5: Effect of point mutations in AeSCP-2 on [^{3}H]palmitic acid uptake in *A. aegypti* Aag-2 cells. Aag-2 cells were transfected with overexpression vectors (see Materials and Methods), and the empty vector was used as a negative control. Overexpression of each protein was verified via Western blotting analysis (Figure 2 of the Supporting Information). The mean and standard deviation are shown ($N = 3$).

DISCUSSION

Ligand Specificity of AeSCP-2. In their natural environment, the dietary sterols on which mosquito larvae feed are mostly various phytosterols in degrading leaf debris (*28*, *29*). Cholesterol is an essential nutrient to insects due to the lack of de novo cholesterol biosynthesis (*28*). The ability of AeSCP-2 to bind β-sitosterol is of interest because *A. aegypti* larvae effectively

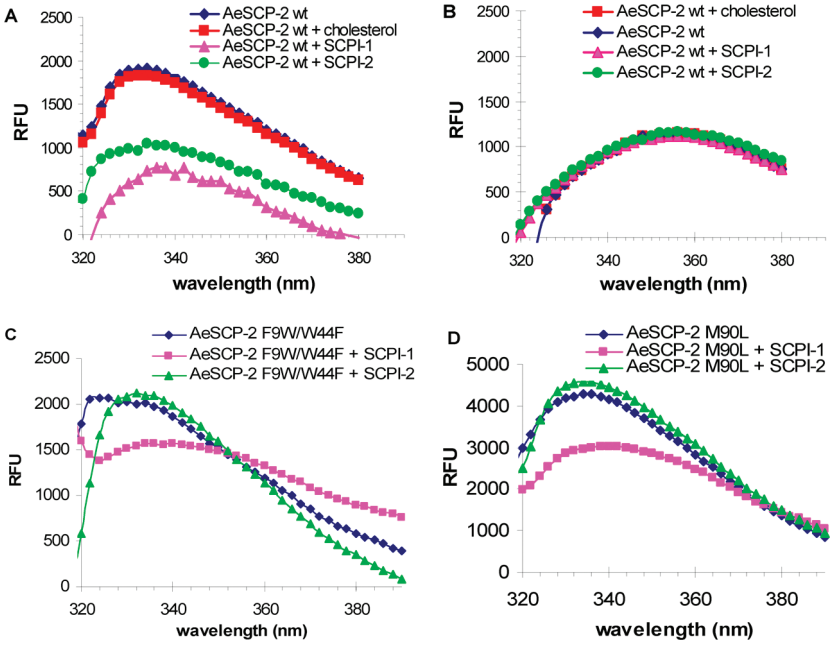

FIGURE 6: Intrinsic tryptophan fluorescence emission in wild-type AeSCP-2 and its mutants. (A) Wild-type AeSCP-2 recombinant proteins in the presence or absence of ligand or inhibitors. (B) Wild-type AeSCP-2 recombinant protein denatured in 50 mM Tris-HCl and 6.5 M GuHCl (pH 7.4) in the presence and absence of ligand or inhibitors. (C) F9W/W44F mutant AeSCP-2 in the presence and absence of inhibitors. (D) M90L mutant AeSCP-2 in the presence and absence of inhibitors.

convert β-sitosterol to cholesterol (*28*), whereas conversion of phytosterols to cholesterol most likely takes place in the insect midgut (*34*−*36*). Furthermore, the level of *AeSCP-2* expression is high in the midgut during the larval feeding stage (*8*). The results suggest that AeSCP-2 may be involved in trafficking of phytosterols in the midgut for conversion to cholesterol. Further experiments are required to verify the involvement of AeSCP-2 in phytosterol conversions in the midgut.

Vertebrate SCP-2 has been shown to stimulate androgen production in adrenal glands (*37*, *38*). In insects, cholesterol is the precursor for the synthesis of ecdysteroids, the insect molting hormones. In the ecdysteroid hormone biosynthesis pathway, cholesterol is first metabolized to 7-dehydrocholesterol in the cytoplasm (*30*). There was speculation that sterol carrier proteins such as SCP-2 may be in involved in the transfer of 7-dehydrocholesterol into mitochondria for ecdysteroid biosynthesis (*30*). We did not detect binding of 7-dehydrocholesterol to wild-type AeSCP-2 *in vitro* (Figure 1 and Table 1). In addition, there is a lack of evidence of AeSCP-2 localizing in the mitochondria (*11*), where steroid biosynthesis takes place. The results suggest that AeSCP-2 may not be involved in the transport of 7-dehydrocholesterol to mitochondria, the early steps in the ecdysteroid biosynthesis (*30*). Surprisingly, single point mutations in AeSCP-2 effectively altered ligand specificity (Table 3). Three sterols examined in this study responded to point mutations in the ligand cavity differently. F32W introduced a bulkier side chain residue into the ligand cavity (Figure 2), yet the mutation enabled 7-dehydrocholesterol to compete with NBD-cholesterol for binding to the protein (Table 3). On the other hand, F32W significantly reduced the affinity of the protein for NBD-cholesterol (Figure 3 and Table 2) and weakened cholesterol binding (Table 3). However, F32W significantly enhanced the competitive binding of β-sitosterol to the protein (Table 3). Binding of sterols in AeSCP-2 has not been resolved at the molecular structural level; therefore, the role of F32 in sterol binding is unknown. It is likely that F32 plays a role in stabilization of the bound sterol ligand. The Y30A mutation is not a conservative substitution (*39*); therefore, it might alter the hydrophobic ligand cavity, allowing 7-dehydrocholesterol binding. The structural difference between cholesterol and 7-dehydrocholesterol is the formation of a double bond in the steroid ring between carbons 7 and 8. It is possible that 7-dehydrocholesterol may adapt a conformation different from that of cholesterol with regard to the trans/cis status of the sterol ring (*40*); therefore, binding of 7-dehydrocholesterol may require a slightly different cavity space that Y30 in AeSCP-2 could not provide. It is noticed that amino acid residues at the equivalent positions in AeSCP-2-like proteins are not conserved in all members of the family (*1*), suggesting that other members of the AeSCP-2-like proteins in the protein family may bind to 7-dehydrocholesterol.

It is possible that W44E and M90L mutations resulted in altered affinity only for cholesterol (Figure 3 and Table 3). This is a likely scenario because palmitic acid and β-sitosterol did not show the same sensitivity to compete with NBD-cholesterol at very low concentrations like that of cholesterol in W44E and M90L mutants (Table 3). Interestingly, AeSCP-2 is the only member of the mosquito SCP-2 protein family that has methionine at the equivalent positions of M90 (*1*), and AeSCP-2 was the only protein among AeSCP-2 and AeSCP-2-like proteins to affect cholesterol uptake *in vivo* [Figure 4 (*2*)]. However, sensitivity to palmitic acid competition with NBD-cholesterol in AeSCP-2 mutants was not impaired in all tested mutants (Table 3). A single point mutation in SCP-2 that alters the sensitivity and may affect the selectivity of sterol ligand has been reported. In the *Ar. thaliana* SCP-2, an M to L mutation at the position equivalent to M90 in AeSCP-2 results in an abolished sterol sensitivity in BODIPY-phosphatidylcholine transfer assays (*20*). The results from single point mutations in AeSCP-2 suggest that sterol ligand selectivity may be strongly influenced by the specific residues in the hydrophobic core, whereas a fatty acid ligand could be accommodated in the ligand cavity with diverse nonpolar amino acid residues.

In the three-dimensional AeSCP-2 protein structure, W44 is only partially buried in the hydrophobic core of AeSCP-2 (Figure 3 of the Supporting Information). In addition, the tryptophan is coordinated by $\pi-\pi$ stacking with phenylalanine (F9) that interacts with ligand (Figure 2 and Figure 3 of the Supporting Information). Changes in this $\pi-\pi$ stacking arrangement may lead to disruption of this region of the ligand cavity and weakening of cholesterol binding. To test the overall sensitivity of this $\pi-\pi$ stacking structure to changes in ligand binding, double mutants in which the tryptophan around the aromatic triad was mutated were created (Figure 2, F9, F32, and W44). The recombinant F32W/W44F protein was unstable when purified, which was determined via dynamic light scattering (*23*) as having $>40\%$ polydispersity. Therefore, a conservative double mutation at those positions in AeSCP-2 may reduce the biological activity. The recombinant F9W/W44F protein had an only moderate effect on binding to NBD-cholesterol (Figure 3 and Table 2), whereas W44A did not affect NBD-cholesterol/cholesterol competition compared to the wild type (Table 3). Therefore, W44 and F9 $\pi-\pi$ stacking may not play a critical role in ligand binding, at least for cholesterol binding to the protein. It must be noted that all mutants, when presented at high concentrations, bound NBD-cholesterol (Figure 3), suggesting that none of the mutations were sufficiently severe to cause complete disruption of the ligand binding.

In Vivo Function of AeSCP-2. Multiple steps are involved in cellular lipid uptake. Lipid carriers such as low-density lipoproteins (LDL in the vertebrate and LDLp in the insects) donate lipids to the extracellular layer of the cytoplasmic membrane where the free lipids flip-flop across the cytoplasm membrane bilayer; cytosolic lipid carriers such as cytosolic fatty acid binding protein and SCP-2 desorb the free lipids from the cytoplasm membrane and deliver the lipids to the site of storage or metabolism (*41*, *42*). There is speculation that the ability to bind cholesterol would be critical for AeSCP-2's *in vivo* function in aiding cholesterol uptake. The correlation between affinity for cholesterol and the ability in transport the cholesterol ligand suggests an important role for AeSCP-2 in cholesterol uptake *in vivo* (Figures 3 and 4). The mechanism underlying AeSCP-2-mediated cellular cholesterol uptake is unclear. AeSCP-2 is not a membrane-bound protein (*11*); therefore, AeSCP-2-mediated lipid absorption is unlike that of the membrane transporters such as Niemann-Pick C1-like 1 (NPC1-L1) (*43*). AeSCP-2 may enhance desorption of membrane-bound ligand through collision with the membrane-bound cholesterol (*15*), which in turn may lead to an enhanced cellular uptake of cholesterol. The SCP-2/membrane collision model is the proposed mode of action for fatty acid transport by SCP-2 of *Yarrowia lipolytica* (*44*). However, the SCP-2/membrane collision model cannot explain AeSCP-2's ligand selectivity in aiding cholesterol but not palmitic acid uptake in cultured mosquito cells (Figures 4 and 5, wt vs empty vector). It has been shown that vertebrate SCP-2 increases

the degree of sterol transfer from the cholesterol-rich membrane domain (*45*). Therefore, the interaction of apo-AeSCP-2 and the cholesterol-rich domains in the cytoplasm membrane may be the key in AeSCP-2-mediated selective desorption of membrane-bound cholesterol, which results in protein-mediated diffusion of cholesterol into the cell. This process may be specifically important to insects because receptor- or lipoprotein-mediated endocytosis and/or exocytosis is not involved in cellular lipid transfer (*46*, *47*). Further studies are needed to shed light on the mechanism of AeSCP-2-mediated selective uptake of cholesterol in mosquito cells.

Understanding the role of ligand specificity is complex with regard to the biological function of members of the *SCP-2* family. In the mouse L-cells, overexpression of SCP-2 did not affect palmitic acid uptake but reduces the rate of uptake of phytanic acid (*48*), whereas it has been shown that SCP-2 overexpression enhances uptake of NBD-stearate, an analogue of the C18 fatty acid (*49*). However, overexpression of wild-type AeSCP-2 or its mutants did not change the levels of radiolabeled palmitic acid incorporation in cultured mosquito cells (Figure 5), consistent with the report that knockdown expression of AeSCP-2 did not affect the uptake of [^{3}H]palmitic acid from the bloodmeal in female adults (*2*). The results suggest that AeSCP-2 may not be involved in cellular palmitic acid uptake in mosquitoes or AeSCP-2 may play an only minor role in cellular palmitic acid uptake. Therefore, binding of a ligand in AeSCP-2 *in vitro* does not predict the *in vivo* role of AeSCP-2 in ligand transport. A similar observation has been reported for another mammalian sterol carrier protein (*26*). *A. aegypti* has the cytosolic fatty acid binding protein (AAEL005997-RA) that may play a major role in protein-mediated desorption of membrane-bound free fatty acid in mosquito cells. Because AeSCP-2 does bind to palmitic acid *in vitro* (*9*) (Figure 1 and Table 1), AeSCP-2 may be involved in other aspects of cellular fatty acid metabolism. Further work is needed to address the biological role of AeSCP-2 in fatty acid metabolism.

We conducted experiments to explore the interaction of inhibitors of cholesterol binding on AeSCP-2 wild type and mutants. A significant quenching of the absorption spectra was observed when either SCPI-1 or SCPI-2 was added to the protein. The differences in quenching tryptophan fluorescence emission between SCP-2 inhibitors-1 and -2 suggested that the inhibitors bind similarly but not identically to the protein. However, this region of the molecular interaction between SCPIs and AeSCP-2 is not affected by bound cholesterol (Figure 5B). Further work is needed to address how SCPIs suppress binding of cholesterol to AeSCP-2 at the molecular level.

In summary, results from the *in vitro* and *in vivo* studies of wild-type and mutant AeSCP-2s presented here further affirm the hypothesis that SCP-2 in *A. aegypti* plays a crucial role in the cellular uptake of cholesterol, an essential nutrient for the insect. Amino acid residues that appear to play critical roles in the proper binding of cholesterol in AeSCP-2 have been identified, both in the ligand cavity and in the overall uptake of cholesterol in live cells.

SUPPORTING INFORMATION AVAILABLE

Quantitative analysis of AeSCP-2 overexpression in Aag-2 cells (Table 1), Western blot analysis of AeSCP-2 overexpression in Aag-2 cells (Figure 1), binding of NBD-cholesterol in recombinant wild-type AeSCP-2 (Figure 2), and partial surface diagrams (Pymol) of AeSCP-2 (Protein Data Bank entry 1PZ4) at 1.35 Å resolution showing $\pi-\pi$ stacking of F9 and W44 (Figure 3). This material is available free of charge via the Internet at http://pubs.acs.org.

REFERENCES

1. Dyer, D. H., Vyazunova, I., Lorch, J. M., Forest, K. T., and Lan, Q. (2009) Characterization of the yellow fever mosquito sterol carrier protein-2 like 3 gene and ligand-bound protein structure. *Mol. Cell. Biochem. 326*, 67–77.
2. Dyer, D. H., Wessely, V., Forest, K. T., and Lan, Q. (2008) Three-dimensional structure/function analysis of SCP-2-like2 reveals differences among SCP-2 family members. *J. Lipid Res. 49*, 644–653.
3. Gallegos, A. M., Atshaves, B. P., Storey, S. M., Starodub, O., Petrescu, A. D., Huang, H., McIntosh, A. L., Martin, G. G., Chao, H., Kier, A. B., and Schroeder, F. (2001) Gene structure, intracellular localization, and functional roles of sterol carrier protein-2. *Prog. Lipid Res. 40*, 498–563.
4. Frolov, A., Cho, T. H., Billheimer, J. T., and Schroeder, F. (1996) Sterol carrier protein-2, a new fatty acyl coenzyme A-binding protein. *J. Biol. Chem. 271*, 31878–31884.
5. Colles, S. M., Woodford, J. K., Moncecchi, D., Myers-Payne, S. C., McLean, L. R., Billheimer, J. T., and Schroeder, F. (1995) Cholesterol interaction with recombinant human sterol carrier protein-2. *Lipids 30*, 795–803.
6. Moncecchi, D., Murphy, E. J., Prows, D. R., and Schroeder, F. (1996) Sterol carrier protein-2 expression in mouse L-cell fibroblasts alters cholesterol uptake. *Biochim. Biophys. Acta 1302*, 110–116.
7. Murphy, E. J. (2002) Sterol carrier protein-2: Not just for cholesterol any more. *Mol. Cell. Biochem. 239*, 87–93.
8. Krebs, K. C., and Lan, Q. (2003) Isolation and expression of a sterol carrier protein-2 gene from yellow fever mosquito, *Aedes aegypti*. *Insect Mol. Biol. 12*, 51–60.
9. Dyer, D. H., Lovell, S., Thoden, J. B., Holden, H. M., Rayment, I., and Lan, Q. (2003) The Structural Determination of an Insect Sterol Carrier Protein-2 with a Ligand-bound C16 Fatty Acid at 1.35-Å Resolution. *J. Biol. Chem. 278*, 39085–39091.
10. Blitzer, E. J., Vyazunova, I., and Lan, Q. (2005) Functional analysis of AeSCP-2 using gene expression knockdown in the yellow fever mosquito, *Aedes aegypti*. *Insect Mol. Biol. 14*, 301–307.
11. Lan, Q., and Massey, R. J. (2004) Subcellular localization of the mosquito sterol carrier protein-2 and sterol carrier protein-x. *J. Lipid Res. 45*, 1468–1474.
12. Kim, M., Wessely, V., and Lan, Q. (2005) Identification of mosquito sterol carrier protein-2 inhibitors. *J. Lipid Res. 46*, 650–657.
13. Seedorf, U., Raabe, M., Ellinghaus, P., Kannenberg, F., Fobker, M., Engel, T., Denis, S., Wouters, F., Wirtz, K. W. A., Wanders, R. J. A., Maeda, N., and Assmann, G. (1998) Defective peroxisomal catabolism of branched fatty acyl coenzyme A in mice lacking the sterol carrier protein-2/sterol carrier protein-x gene function. *Genes Dev. 12*, 1189–1201.
14. Fuchs, M., Hafer, A., Münch, C., Kannenberg, F., Teichmann, S., Scheibner, J., Stange, E. F., and Seedorf, U. (2001) Disruption of the Sterol Carrier Protein 2 Gene in Mice Impairs Biliary Lipid and Hepatic Cholesterol Metabolism. *J. Biol. Chem. 276*, 48058–48065.
15. Leventis, R, and Silvius, J. R. (2001) Use of Cyclodextrins to Monitor Transbilayer Movement and Differential Lipid Affinities of Cholesterol. *Biophys. J. 81*, 2257–2267.
16. Phillips, M. C., Johnson, W. J., and Rothblat, G. H. (1987) Mechanisms and consequences of cellular cholesterol exchange and transfer. *Biochim. Biophys. Acta 906*, 223–276.
17. Rodrigueza, W. V., Phillips, M. C., and Williams, K. J. (1998) Structural and metabolic consequences of liposome−lipoprotein interactions. *Adv. Drug Delivery Rev. 32*, 31–43.
18. Atshaves, B. P., Gallegos, A. M., McIntosh, A. L., Kier, A. B., and Schroeder, F. (2003) Sterol Carrier Protein-2 Selectively Alters Lipid Composition and Cholesterol Dynamics of Caveolae/Lipid Raft vs Nonraft Domains in L-Cell Fibroblast Plasma Membranes. *Biochemistry 42*, 14583–14598.
19. Huang, H., Gallegos, A. M., Zhou, M., Ball, J. M., and Schroeder, F. (2002) Role of the Sterol Carrier Protein-2 N-Terminal Membrane Binding Domain in Sterol Transfer. *Biochemistry 41*, 12149–12162.
20. Viitanen, L., Nylund, M., Eklund, D. M., Alm, C., Eriksson, A.-K., Tuuf1, J., Salminen, T. A., Mattjus, P., and Edqvist, J. (2006) Characterization of SCP-2 from *Euphorbia lagascae* reveals that a single Leu/Met exchange enhances sterol transfer activity. *FEBS J. 273*, 5641–5655.

21. Peleg, J. (1968) Growth of Arboviruses In Primary Tissue Culture of *Aedes Aegypti* Embryos. *Am. J. Trop. Med. Hyg. 17*, 219–223.
22. Lan, Q., and Fallon, M. (1990) Small heat shock proteins distinguish between two mosquito species and confirm identity of their cell lines. *Am. J. Trop. Med. Hyg. 43*, 669–676.
23. Zulauf, M., and D'Arcy, A. (1992) Light scattering of proteins as a criterion for crystallization. *J. Cryst. Growth 122*, 102–106.
24. Lan, Q., Gerenday, A., and Fallon, A. M. (1993) Cultured *Aedes albopictus* mosquito cells synthesize hormone-inducible proteins. *In Vitro Cell. Dev. Biol. 29A*, 813–818.
25. Lakowicz, J. R. (1980) Fluorescence spectroscopic investigations of the dynamic properties of proteins, membranes and nucleic acids. *J. Biochem. Biophys. Methods 2*, 91–119.
26. Andersen, J., Olsen, L., Hansen, K. B., Taboureau, O., Jørgensen, F. S., Jørgensen, A. M., Bang-Andersen, B., Egebjerg, J., Strømgaard, K., and Kristensen, A. S. (2010) Mutational mapping and modeling of the binding site for (S)-citalopram in the human serotonin transporter. *J. Biol. Chem. 285*, 2051–2063.
27. Baker, B. Y., Epand, R. F., Epand, R. M., and Miller, W. L. (2007) Cholesterol Binding Does Not Predict Activity of the Steroidogenic Acute Regulatory Protein, StAR. *J. Biol. Chem. 282*, 10223–10232.
28. Svoboda, J. A., Thompson, M. J., Herbert, E. W., Jr., Shortino, T. J., and Szczepanik-Vanleeuwen, P. A. (1982) Utilization and Metabolism of Dietary Sterols in the Honey Bee and the Yellow Fever Mosquito. *Lipids 17*, 220–225.
29. Warner, S. A., Sovocool, G. W., Domnas, A. J., and Jaronski, S. T. (1984) The Composition of Sterols in Mosquito Larvae Is Optimal for Zoosporogenesis in *Lagenidium giganteum*. *J. Invertebr. Pathol. 43*, 293–296.
30. Grieneisen, M. L., Warren, J. T., and Gilbert, L. I. (1993) Early Steps in Ecdysteroid Biosynthesis: Evidence for the Involvement of Cytochrome P-450 Enzymes. *Insect Biochem. Mol. Biol. 23*, 13–23.
31. Vyazunova, I., and Lan, Q. (2008) Insect sterol carrier protein-2 gene family: Structures and functions. Chapter 11. In Recent Advances in Insect Physiology, Toxicology and Molecular Biology (Liu, N., Ed.) pp 173−198, Research Signpost, Kerala, India.
32. Reshetnyak, Y. K., and Burstein, E. A. (2001) Decomposition of Protein Tryptophan Fluorescence Spectra into Log-Normal Components. II. The Statistical Proof of Discreteness of Tryptophan Classes in Proteins. *Biophys. J. 81*, 1710–1734.
33. Larson, R. T., Wessely, V., Jiang, Z., and Lan, Q. (2008) Larvicidal activity of sterol carrier protein-2 inhibitor in four species of mosquitoes. *J. Med. Entomol. 45*, 439–444.
34. Dwivedy, A. K. (1985) Dietary cholesterol utilization by the housefly, *Musca domestica*. *Insect Biochem. Mol. Biol. 15*, 137–140.
35. Kuthiala, A., and Ritter, K S. (1988) Esterification of cholesterol and cholestanol in the whole body, tissues, and frass of *Heliothis zea*. *Arch. Insect Biochem. Physiol. 7*, 237–248.
36. Komnick, H., and Giesa, U. (1994) Intestinal absorption of cholesterol, transport in the haemolymph, and incorporation into the fat body and Malpighian tubules of the larval dragonfly *Aeshna cyanea*. *Comp. Biochem. Physiol. 107*, 553–557.
37. McNamara, B. C., and Jefcoate, C. R. (1989) The role of sterol carrier protein 2 in stimulation of steroidogenesis in rat adrenal mitochondria by adrenal cytosol. *Arch. Biochem. Biophys. 75*, 53–62.
38. Mendis-Handagama, S. M., Aten, R. F., Watkins, P. A., Scallen, T. J., and Berhman, H. R. (1995) Peroxisomes and sterol carrier protein-2 in luteal cell steroidogenesis: A possible role in cholesterol transport from lipid droplets to mitochondria. *Tissue Cell 27*, 483–490.
39. Hentikoff, S., and Hentikoff, J. G. (1992) Amino acid substitution matrices from protein blocks. *Proc. Natl. Acad. Sci. U.S.A. 89*, 10915–10919.
40. Tantuco, D. E., and Csizmadia, I. G. (2000) Stabilities for the eight isomeric forms of the steroid skeleton (perhydrocyclopentanophenanthrene). *THEOCHEM 503*, 97–111.43.
41. Stremmel, W., Pohl, L., Ring, A., and Herrmann, T. (2001) A new concept of cellular uptake and intracellular trafficking of long-chain fatty acids. *Lipids 36*, 981–989.
42. Maxfield, F. R., and Menon, A. K. (2006) Intracellular sterol transport and distribution. *Curr. Opin. Cell Biol. 18*, 379–385.
43. Wang, J., Chu, B. B., Ge, L., Li, B. L., Yan, Y., and Song, B. L. (2009) Membrane topology of human NPC1L1, a key protein in enterohepatic cholesterol absorption. *J. Lipid Res. 50*, 1653–1662.
44. Falomir-Lockhart, L. J., Burgardt, N. I., Ferreyra, R. G., Ceolin, M., Ermácora, M. R., and Córsico, B. (2009) Fatty acid transfer from *Yarrowia lipolytica* sterol carrier protein 2 to phospholipid membranes. *Biophys. J. 97*, 248–256.
45. Gallegos, A. M., McIntosh, A. L., Atshaves, B. P., and Schroeder, F. (2004) Structure and cholesterol domain dynamics of an enriched caveolae/raft isolate. *Biochem. J. 382*, 451–461.
46. Jouni, Z. E., McGill, B., and Wells, M. A. (2002) β-Cyclodextrin facilitates cholesterol efflux from larval *Manduca sexta* fat body and midgut in vitro. *Comp. Biochem. Physiol., Part B: Biochem. Mol. Biol. 132*, 699–709.
47. Atshaves, B. P., Storey, S. M., Petrescu, A., Greenberg, C. C., Lyuksyutova, O. I., Smith, R., III, and Schroeder, F. (2002) Expression of fatty acid binding proteins inhibits lipid accumulation and alters toxicity in L cell fibroblasts. *Am. J. Physiol. 283*, C688–C703.
48. Atshaves, B. P., Storey, S. M., and Schroeder, F. (2003) Sterol carrier protein-2/sterol carrier protein-x expression differentially alters fatty acid metabolism in L cell fibroblasts. *J. Lipid Res. 44*, 1751–1762.
49. Murphy, E. J. (1998) Sterol carrier protein-2 expression increases NBD-stearate uptake and cytoplasmic diffusion in L cells. *Am. J. Physiol. 275*, G237–G243.